RSC Advances

PAPER

View Article Online
View Journal | View Issue

Cite this: *RSC Adv.*, 2019, **9**, 41868

Immobilized TiO_2 nanoparticles on carbon nanotubes: an efficient heterogeneous catalyst for the synthesis of chromeno[*b*]pyridine derivatives under ultrasonic irradiation†

Shahrzad Abdolmohammadi, *[a] Behrooz Mirza[b] and Esmail Vessally[c]

Received 1st November 2019
Accepted 11th December 2019

DOI: 10.1039/c9ra09031b

rsc.li/rsc-advances

A new protocol for the synthesis of chromeno[*b*]pyridine derivatives is described *via* a three-component reaction of 4-aminocoumarin, aromatic aldehydes and malononitrile catalyzed by TiO_2 nanoparticles immobilized on carbon nanotubes (TiO_2-CNTs) as an efficient heterogeneous catalyst under ultrasonic irradiation in water. The sustainable and economic benefits of the protocol are the high yields of products, short reaction time, simple work-up procedure, and use of a non-toxic and reusable catalyst.

1. Introduction

The chromene nucleus is a well-known favored structure motif, common and significant feature of a variety of natural products and medicinal agnates.[1] Compounds containing the chromene motif have been successfully used as cosmetics, pigments[2] and potential biodegradable agrochemicals.[3] These compounds exhibit a wide range of interesting biological activities such as antimicrobial,[4] antiviral,[5,6] antitumoral,[7] mutagenicitical,[8] antiproliferative,[9] sex pheromonal,[10] antioxidant,[11] enzyme inhibitoring,[12] and central nervous system active drugs.[13] Moreover, compounds incorporating chromene core structures are most prevalent among natural bio-active compounds. For example uvafzlelin, as a naturally occurring 4*H*-chromene isolated from the stems of *Uvaria ufielii*, can be regarded as antimicrobial against Gram-positive and acid-fast bacteria,[14] conrauinone A extracted from the bark of the tree *Millettia conraui* is useful in the treatment of intestinal parasites,[15] and erysenegalensein C has been isolated from the bark of *Erythrina senegalensis* and is recognized as a drug for the treatment of stomach pain, female infertility and gonorrhoea (Fig. 1).[16]

During the past decade, the utility of metal oxide nanoparticles (NPs) as efficient heterogeneous catalysts has become increasingly important aim of the organic researches in the synthesis of organic compounds. The remarkable features of these catalysts are extremely dealing with the size and shape dependent unusual physical and chemical properties.[17–20] Amongst many metal oxide nanoparticles, recently titanium dioxide nanoparticles (TiO_2 NPs) have been successfully employed in numerous catalytic organic and inorganic transformations due to the salient features such as high catalytic activity, non-toxicity, easy availability, moisture stability and reusability.[21–28] Furthermore, carbon nanotubes (CNTs) have been emerged as promising support materials for a variety of heterogeneous nanoparticle catalysts because of their unique properties such as high quality active sites, excellent electron conductivity, chemical inertness, and retardation of electron–hole recombination.[29,30] Based on, the pioneer studies of supported metal nanoparticles, the catalytic potential of TiO_2 nanoparticles immobilized on carbon nanotubes (TiO_2-CNTs) can be significantly improved due to their modified structural, chemical, electrical, and optical properties.[31,32]

Current interests in the sustainable chemistry,[33] include elaborate design and development of sequences in the synthesis of alternative molecular scaffolds while combining structural diversity with eco-congeniality, are remarkable challenges for organic chemists.[34] In this broad field of research, the multicomponent reactions (MCRs),[35] due to their ability to combine three or more reactant molecules in a single operation to construct one product containing substantial elements of all the reactants[36,37] are well-established tools to achieve this near ideal goal.[38–42]

The use of organic solvents which is often a constitutive part of chemical or another industrial manufacturing process is mainly causing environmental pollution. According to this, attempts have been made to develop the cleaner processes using alternate energy sources and green reaction media in organic synthesis and industry. Replacing water as an ideal green medium with other popular reaction solvents, has gained increasing interest for proper practice of green chemistry because it is safe, non-toxic, unquestionably cheap and readily

[a]*Department of Chemistry, East Tehran Branch, Islamic Azad University, P. O. Box 18735-138, Tehran, Iran. E-mail: s.abdolmohamadi@yahoo.com; s.abdolmohamadi@iauet.ac.ir; Fax: +98 21 3358 4011; Tel: +98 21 3359 4950*

[b]*Department of Chemistry, Karaj Branch, Islamic Azad University, Karaj, Tehran, Iran*

[c]*Department of Chemistry, Payame Noor University, Tehran, Iran*

† Electronic supplementary information (ESI) available. See DOI: 10.1039/c9ra09031b

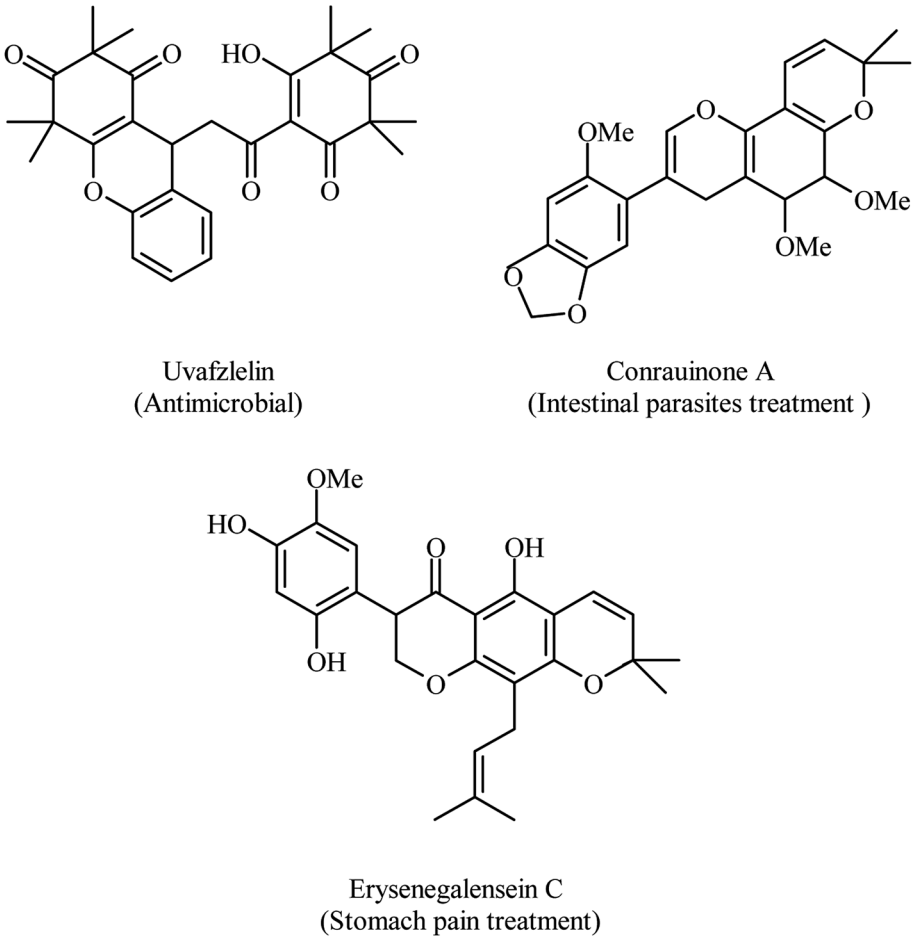

Fig. 1 Natural biologically active compounds containing fused chromenes.

available.[43–47] Furthermore, ultrasound can be also selected as an alternate greener approach due to its pronounced features such as improvement of reaction rates, formation of pure products in high yields and easier operation.[48–50] The efficiency of sonochemistry as an innovative and powerful technique in accelerating organic transformations has been preferably expanded in several different fields of organic chemistry.[51–54]

We have recently developed some TiO_2-CNTs catalyzed sustainable synthetic procedures leading to heterocyclic compounds.[55–57] In the present work, we set out to test the efficiency of TiO_2-CNTs as a reusable and neutral heterogeneous catalyst in a novel and practical approach for the preparation of 2-amino-5-oxo-4-aryl-5*H*-chromeno[4,3-*b*]pyridin-3-yl cyanides **4(a–l)** *via* a three-component reaction of 4-aminocoumarin (**1**), aromatic aldehydes (**2**), and malononitrile (**3**) in aqueous media under ultrasonic irradiation (Scheme 1).

2. Experimental

2.1. Materials and methods

All of the chemical materials used in this work were purchased from Merck and Fluka and used without further purification. Melting points were determined on an Electrothermal 9100 apparatus. IR spectra were obtained on an ABB FT-IR (FTLA 2000) spectrometer. ^{1}H NMR and ^{13}C NMR spectra were recorded on a Bruker DRX-500 AVANCE at 500 and 125 MHz respectively, using TMS as internal standard and DMSO (D6) as solvent. Elemental analyses were carried out on Foss-Heraeus CHN–O-rapid analyzer instruments. The microscopic morphology of the catalyst was revealed using scanning electron microscope (SEM, Philips, XL-30) equipped with an energy dispersive X-ray detector (EDX). The transmission electron microscopy (TEM) image of the catalyst was obtained on a Philips EM208 transmission electron microscope under acceleration. Powder X-ray diffraction data were determined on a Rigaku D-max C III, X-ray Diffractometer using Cu Kα radiation (λ = 1.54 Å). Ultrasonication was performed using on a multiwave ultrasonic generator (Sonicator 3200; Bandelin, MS 73), equipped with a converter/transducer and titanium oscillator (horn), 12.5 mm in diameter, with an operation frequency of 20 KHz with a maximum power output of 200 W.

2.2. General procedure for the synthesis of TiO_2-CNTs nanocomposite

The nanocomposite was synthesized by a simple sonochemical method.[58] Multi walled carbon nanotubes (MWCNTs) (0.1 g)

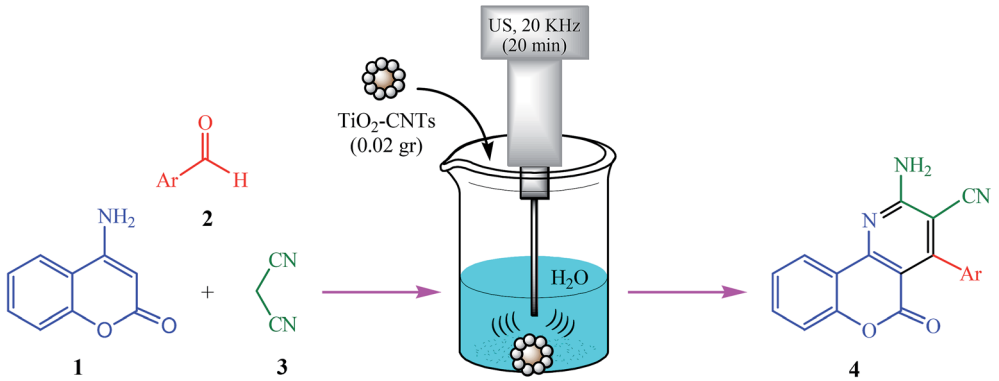

Scheme 1 Ultrasound-assisted, TiO_2-CNTs catalyzed preparation of 2-amino-5-oxo-4-aryl-5*H*-chromeno[4,3-*b*]pyridin-3-yl cyanides in water.

were dispersed in the mixture of solution of tetraethylorthotitanat (0.3 g) in 200 mL acetone with the aid of ultrasonication for 2 h. Further, sodium dodecyl sulfate (SDS) (0.04 g) was added as a shape controller to the above mixture. Hydrolysis was occurred rapidly when obtained mixture was poured into deionized water (200 mL). Subsequently, the produced precipitate was vacuum-filtered, washed with ethanol and dried in a vacuum oven at 77 °C for about 20 h. Finally, calcination of the resulting solid at 400 °C (heating rate: 1 °C min^{-1}) for 30 minutes in an oven, gave the TiO_2-CNTs nanocomposite powder.

2.3. General procedure for the preparation of compounds 4a–l

A mixture of 4-aminocoumarin (**1**, 1 mmol), aromatic aldehyde **2** (1 mmol), malononitrile (**3**, 1.2 mmol) and TiO_2-CNTs nanocomposite (0.02 g) in H_2O (3 mL) was sonicated at room temperature for 20 min in a beaker equipped with ultrasonic probe under the power of 60 W. The reaction progress was monitored by TLC using 3 : 1 ethyl acetate/*n*-hexane as an eluent. After completion of the reaction, the reaction was allowed to stand for 10 min at room temperature, and then the solid obtained was filtered. The residue was then dissolved in hot ethanol (3 mL) and the catalyst was removed for reusing by centrifuging, washing with ethanol, and drying in an oven. The pure product was obtained by cooling the ethanol solution to room temperature, diluted with 1 mL H_2O and allowed to crystallize.

2.4. Selected spectroscopic data

2-Amino-5-oxo-4-phenyl-5*H*-chromeno[4,3-*b*]pyridin-3-yl cyanide (4a). White solid, yield: 0.295 g (94%), mp = 302–304 °C. IR (KBr): ν_{max} 3380, 3267, 2189, 1717, 1676, 1606 cm^{-1}. ^{1}H NMR (500 MHz, DMSO-d_6): 7.31 (2H, br d, J = 8.4 Hz, H_{Ar}), 7.36 (2H, br s, H_{Ar}), 7.38 (2H, br s, NH_2), 7.45 (1H, d, J = 7.4 Hz, H_{Ar}), 7.50 (1H, t, J = 7.6 Hz, H_{Ar}), 7.71 (2H, t, J = 8.3 Hz, H_{Ar}), 7.93 (1H, d, J = 7.7 Hz, H_{Ar}) ppm. ^{13}C NMR (125 MHz, DMSO-d_6): δ 78.6, 103.4, 113.8, 117.4, 119.9, 123.4, 125.4, 129.3, 130.5, 132.0, 133.7, 141.1, 143.1, 150.2, 154.4, 162.0, 167.3 ppm. Anal. calcd for $C_{19}H_{11}N_3O_2$ (313.31): C, 72.84; H, 3.54; N, 13.41. Found: C, 72.94; H, 3.41; N, 13.33.

2-Amino-4-(3-chlorophenyl)-5-oxo-5*H*-chromeno[4,3-*b*]pyridin-3-yl cyanide (4b). White solid, yield: 0.323 g (93%), mp = 287–289 °C. IR (KBr): ν_{max} 3382, 3319, 2192, 1719, 1674, 1606 cm^{-1}. ^{1}H NMR (500 MHz, DMSO-d_6): δ 7.25 (3H, m, H_{Ar}), 7.31 (1H, d, J = 7.8 Hz, H_{Ar}), 7.34 (1H, br s, H_{Ar}), 7.43 (2H, br s, NH_2), 7.45 (1H, d, J = 8.3 Hz, H_{Ar}), 7.71 (1H, t, J = 7.9 Hz, H_{Ar}), 7.91 (1H, d, J = 8.0 Hz, H_{Ar}) ppm. ^{13}C NMR (125 MHz, DMSO-d_6): δ 78.9, 104.8, 114.1, 118.4, 120.1, 123.4, 125.5, 128.5, 132.7, 133.4, 133.8, 138.2, 140.6, 141.7, 144.2, 153.0, 154.3, 163.4, 169.0 ppm. Anal. calcd for $C_{19}H_{10}ClN_3O_2$ (347.76): C, 65.62; H, 2.90; N, 12.08. Found: C, 65.53; H, 2.78; N, 11.91.

2-Amino-4-(2,4-dichlorophenyl)-5-oxo-5*H*-chromeno[4,3-*b*]pyridin-3-yl cyanide (4c). White solid, yield: 0.355 g (93%), mp = 296–298 °C. IR (KBr): ν_{max} 3419, 3280, 2197, 1715, 1674, 1590 cm^{-1}. ^{1}H NMR (500 MHz, DMSO-d_6): δ 7.37 (2H, m, H_{Ar}), 7.43 (2H, br s, NH_2), 7.49 (3H, m, H_{Ar}), 7.73 (1H, t, J = 7.1 Hz, H_{Ar}), 7.95 (1H, d, J = 7.1 Hz, H_{Ar}) ppm. ^{13}C NMR (125 MHz, DMSO-d_6): δ 79.7, 102.2, 113.4, 117.5, 120.1, 123.3, 125.6, 130.0, 132.2, 134.0, 135.2, 138.0, 139.1, 140.6, 142.7, 153.4, 155.5, 162.3, 170.0 ppm. Anal. calcd for $C_{19}H_9Cl_2N_3O_2$ (382.20): C, 59.71; H, 2.37; N, 11.00. Found: C, 59.87; H, 2.24; N, 11.11.

2-Amino-4-(4-cyanophenyl)-5-oxo-5*H*-chromeno[4,3-*b*]pyridin-3-yl cyanide (4d). White solid, yield: 0.321 g (95%), mp = 300–302 °C. IR (KBr): ν_{max} 3483, 3428, 2234, 2197, 1718, 1676, 1601 cm^{-1}. ^{1}H NMR (500 MHz, DMSO-d_6): δ 7.49 (1H, d, J = 8.2 Hz, H_{Ar}), 7.52 (1H, t, J = 7.8 Hz, H_{Ar}), 7.57 (2H, br s, NH_2), 7.60 (2H, d, J = 8.2 Hz, H_{Ar}), 7.74 (1H, t, J = 7.7 Hz, H_{Ar}), 7.91 (1H, d, J = 7.8 Hz, H_{Ar}), 8.18 (2H, d, J = 8.2 Hz, H_{Ar}) ppm. ^{13}C NMR (125 MHz, DMSO-d_6): δ 78.8, 103.6, 113.8, 115.6, 117.5, 119.7, 120.5, 123.4, 125.6, 130.0, 133.4, 141.1, 143.1, 144.4, 153.1, 154.8, 162.4, 169.6 ppm. Anal. calcd for $C_{20}H_{10}N_4O_2$ (338.32): C, 71.00; H, 2.98; N, 16.56. Found: C, 71.14; H, 3.08; N, 16.71.

2-Amino-4-(4-fluorophenyl)-5-oxo-5*H*-chromeno[4,3-*b*]pyridin-3-yl cyanide (4e). White solid, yield: 0.318 g (96%), mp = 256–258 °C. IR (KBr): ν_{max} 3391, 3311, 2199, 1712, 1676, 1606 cm^{-1}. ^{1}H NMR (500 MHz, DMSO-d_6): δ 7.29 (2H, d, J = 8.0 Hz, H_{Ar}), 7.30 (1H, d, J = 7.8 Hz, H_{Ar}), 7.43 (2H, br s, NH_2), 7.49 (2H, d, J = 8.0 Hz, H_{Ar}), 7.52 (1H, d, J = 7.9 Hz, H_{Ar}), 7.73 (1H, t, J = 7.8 Hz, H_{Ar}), 7.94 (1H, d, J = 7.7 Hz, H_{Ar}) ppm. ^{13}C

NMR (125 MHz, DMSO-d_6): δ 78.6, 104.2, 113.8, 117.4, 119.8, 121.1, 123.4, 130.8, 132.2, 133.8, 139.0, 143.6, 150.1, 158.9, 161.8, 169.9 ppm. Anal. calcd for $C_{19}H_{10}FN_3O_2$ (331.30): C, 68.88; H, 3.04; N, 12.68. Found: C, 68.71; H, 2.92; N, 12.82.

2-Amino-4-(3-hydroxyphenyl)-5-oxo-5*H*-chromeno[4,3-*b*] pyridin-3-yl cyanide (4f). White solid, yield: 0.310 g (94%), mp = 292–294 °C. IR (KBr): ν_{max} 3432, 3325, 3229, 2202, 1703, 1672, 1531, 1349 cm^{-1}. ^1H NMR (500 MHz, DMSO-d_6): δ 7.47 (1H, d, J = 8.3 Hz, H_{Ar}), 7.51 (1H, t, J = 7.6 Hz, H_{Ar}), 7.56 (2H, br s, NH_2), 7.64 (1H, t, J = 7.9 Hz, H_{Ar}), 7.73 (1H, t, J = 8.5 Hz, H_{Ar}), 7.82 (1H, d, J = 7.7 Hz, H_{Ar}), 7.92 (1H, d, J = 8.1 Hz, H_{Ar}), 8.13 (1H, br s, H_{Ar}), 8.15 (1H, m, H_{Ar}), 9.24 (1H, s, OH) ppm. ^{13}C NMR (125 MHz, DMSO-d_6): δ 77.8, 103.7, 113.8, 116.1, 117.4, 118.0, 119.8, 120.1, 123.3, 125.4, 134.0, 135.6, 140.6, 144.0, 149.9, 154.8, 159.0, 161.2, 170.0 ppm. Anal. calcd for $C_{19}H_{11}N_3O_3$ (329.31): C, 69.30; H, 3.37; N, 12.76. Found: C, 69.39; H, 3.23; N, 12.88.

2-Amino-4-(4-hydroxyphenyl)-5-oxo-5*H*-chromeno[4,3-*b*] pyridin-3-yl cyanide (4g). White solid, yield: 0.313 g (95%), mp = 285–287 °C. IR (KBr): ν_{max} 3508, 3404, 3286, 2196, 1707, 1670, 1606 cm^{-1}. ^1H NMR (500 MHz, DMSO-d_6): δ 6.71 (2H, d, J = 8.1 Hz, H_{Ar}), 7.07 (2H, d, J = 8.2 Hz, H_{Ar}), 7.37 (2H, br s, NH_2), 7.46 (1H, d, J = 7.9 Hz, H_{Ar}), 7.50 (1H, t, J = 7.8 Hz, H_{Ar}), 7.71 (1H, t, J = 7.7 Hz, H_{Ar}), 7.90 (1H, d, J = 7.6 Hz, H_{Ar}), 9.27 (1H, s, OH) ppm. ^{13}C NMR (125 MHz, DMSO-d_6): δ 79.3, 105.3, 113.9, 116.1, 117.3, 120.3, 123.2, 125.4, 133.6, 134.6, 140.9, 143.8, 150.5, 155.0, 158.4, 160.4, 171.1 ppm. Anal. calcd for $C_{19}H_{11}N_3O_3$ (329.31): C, 69.30; H, 3.37; N, 12.76. Found: C, 69.17; H, 3.48; N, 12.84.

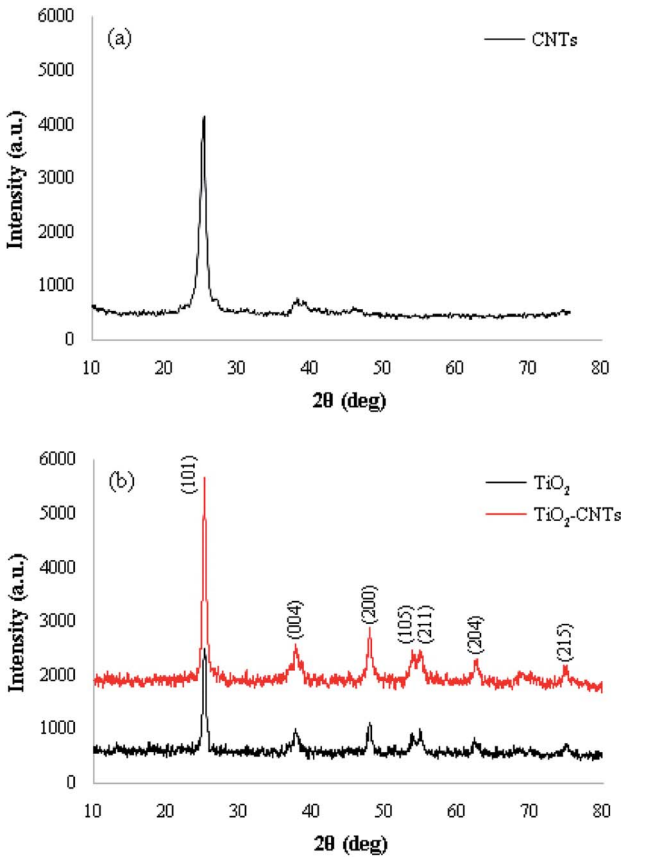

Fig. 2 XRD patterns of (a) CNTs, (b) TiO_2 NPs and TiO_2-CNTs nanocomposite.

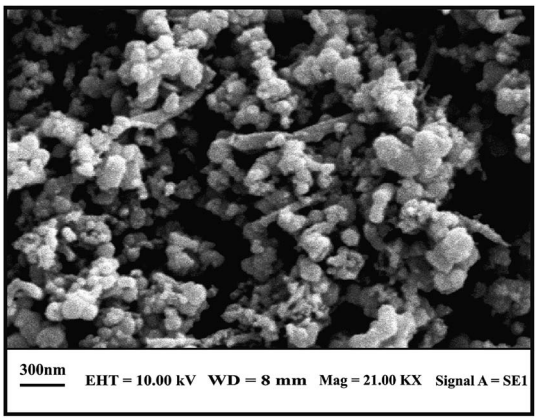

Fig. 3 SEM image of TiO_2-CNTs nanocomposite.

2-Amino-4-(4-methoxyphenyl)-5-oxo-5*H*-chromeno[4,3-*b*] pyridin-3-yl cyanide (4h). Brick-red solid, yield: 0.330 g (96%), mp = 278–280 °C. IR (KBr): ν_{max} 3374, 3313, 2992, 2199, 1699, 1670, 1608 cm^{-1}.^1H NMR (500 MHz, DMSO-d_6): δ 3.76 (3H, s, OCH_3), 7.20 (2H, d, J = 8.1 Hz, H_{Ar}), 7.40 (2H, br s, NH_2), 7.50 (2H, d, J = 8.1 Hz, H_{Ar}), 7.76 (1H, d, J = 7.8 Hz, H_{Ar}), 7.80 (1H, t, J = 7.8 Hz, H_{Ar}), 8.03 (1H, t, J = 7.7 Hz, H_{Ar}), 8.22 (1H, d, J = 7.7 Hz, H_{Ar}) ppm. ^{13}C NMR (125 MHz, DMSO-d_6): δ 55.7, 79.1, 103.1, 113.6, 116.7, 117.4, 120.2, 123.3, 133.7, 136.3, 138.7, 140.9, 143.9, 150.5, 153.9, 159.2, 161.9, 168.4 ppm. Anal. calcd for $C_{20}H_{13}N_3O_3$ (343.34): C, 70.00; H, 3.82; N, 12.24. Found: C, 70.13; H, 3.92; N, 12.13.

2-Amino-4-(4-methylphenyl)-5-oxo-5*H*-chromeno[4,3-*b*] pyridin-3-yl cyanide (4i). White solid, yield: 0.311 g (95%), mp = 291–293 °C. IR (KBr): ν_{max} 3465, 3305, 2879, 2199, 1707, 1674, 1600 cm^{-1}.^1H NMR (500 MHz, DMSO-d_6): δ 2.27 (3H, s, CH_3), 7.37 (2H, m, H_{Ar}), 7.41 (2H, br s, NH_2), 7.46 (1H, d, J = 8.3 Hz, H_{Ar}), 7.51 (1H, t, J = 7.6 Hz, H_{Ar}), 7.56 (2H, br s, H_{Ar}),7.73 (1H, t, J = 7.6 Hz, H_{Ar}), 7.92 (1H, d, J = 8.3 Hz, H_{Ar}) ppm. ^{13}C NMR (125 MHz, DMSO-d_6): δ 20.9, 77.1, 103.4, 113.7, 117.5, 118.4, 120.6,

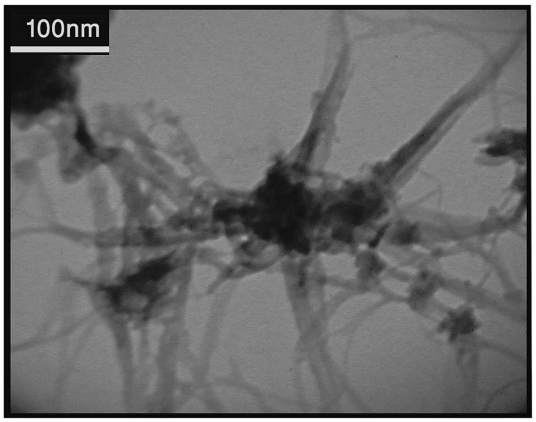

Fig. 4 TEM image of TiO_2-CNTs nanocomposite.

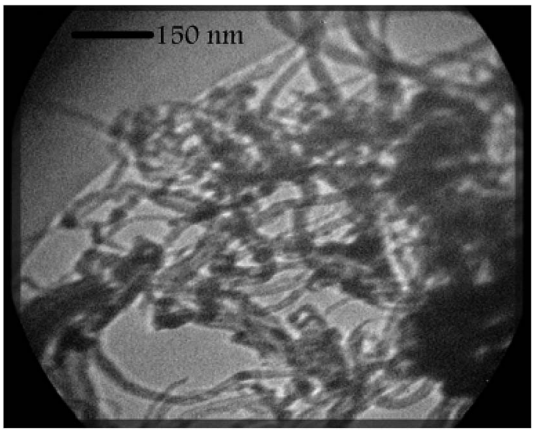

Fig. 5 TEM image of CNTs nanocomposite.

123.4, 133.9, 134.2, 138.7, 140.3, 143.1, 150.7, 155.1, 159.1, 160.5, 169.8 ppm. Anal. calcd for $C_{20}H_{13}N_3O_2$ (327.34): C, 73.39; H, 4.00; N, 12.84. Found: C, 73.54; H, 4.20; N, 12.67.

2-Amino-4-(3-nitrophenyl)-5-oxo-5*H*-chromeno[4,3-*b*] pyridin-3-yl cyanide (4j). Yellow solid, yield: 0.344 g (96%), mp = 284–286 °C. IR (KBr): ν_{max} 3462, 3324, 2209, 1713, 1672, 1606, 1489, 1384 cm^{-1}. ^1H NMR (500 MHz, DMSO-d_6): δ 6.68 (2H, d, J = 7.7 Hz, H_{Ar}), 6.71 (1H, d, J = 7.6 Hz, H_{Ar}), 7.11 (1H, t, J = 7.7 Hz, H_{Ar}), 7.41 (2H, br s, NH_2), 7.46 (1H, d, J = 8.4 Hz, H_{Ar}), 7.49 (1H, t, J = 7.6 Hz, H_{Ar}), 7.70 (1H, t, J = 8.2 Hz, H_{Ar}), 7.91 (1H, d, J = 8.2 Hz, H_{Ar}) ppm. ^{13}C NMR (125 MHz, DMSO-d_6): δ 78.9, 105.0, 113.8, 118.1, 120.1, 121.2, 123.3, 125.6, 130.4, 133.0, 133.8, 140.6, 141.3, 145.6, 147.4, 153.0, 154.1, 162.9, 170.3 ppm. Anal. calcd for $C_{19}H_{10}N_4O_4$ (358.31): C, 63.69; H, 2.81; N, 15.64. Found: C, 63.51; H, 2.93; N, 15.54.

2-Amino-4-(4-pyridyl)-5-oxo-5*H*-chromeno[4,3-*b*]pyridin-3-yl cyanide (4k). Yellow solid, yield: 0.302 g (96%), mp = 289–291 °C. IR (KBr): ν_{max} 3432, 3326, 2193, 1717, 1672, 1613, 1607, 1601 cm^{-1}. ^1H NMR (500 MHz, DMSO-d_6): δ 7.47 (2H, d, J = 8.1 Hz, H_{Ar}), 7.51 (2H, br s, H_{Ar}), 7.53 (2H, br s, NH_2), 7.74 (1H, t, J = 7.8 Hz, H_{Ar}), 7.79 (2H, d, J = 8.1 Hz, H_{Ar}), 8.00 (1H, d, J = 7.8 Hz, H_{Ar}) ppm. ^{13}C NMR (125 MHz, DMSO-d_6): δ 77.8, 103.7, 113.8, 117.5, 119.8, 123.4, 129.8, 133.4, 140.8, 143.9, 146.2, 148.1, 149.6, 153.1, 162.4, 169.8 ppm. Anal. calcd for $C_{18}H_{10}N_4O_2$ (314.30): C, 68.79; H, 3.21; N, 17.83. Found: C, 68.90; H, 3.33; N, 17.93.

2-Amino-4-(2-thiophenyl)-5-oxo-5*H*-chromeno[4,3-*b*]pyridin-3-yl cyanide (4l). White solid, yield: 0.303 g (95%), mp = 280–282 °C. IR (KBr): ν_{max} 3404, 3299, 2192, 1711, 1676, 1608, 1588, 1525 cm^{-1}. ^1H NMR (500 MHz, DMSO-d_6): δ 7.23 (2H, m, H_{Ar}), 7.28 (2H, br s, H_{Ar}), 7.33 (1H, t, J = 8.3 Hz, H_{Ar}), 7.43 (2H, br s,

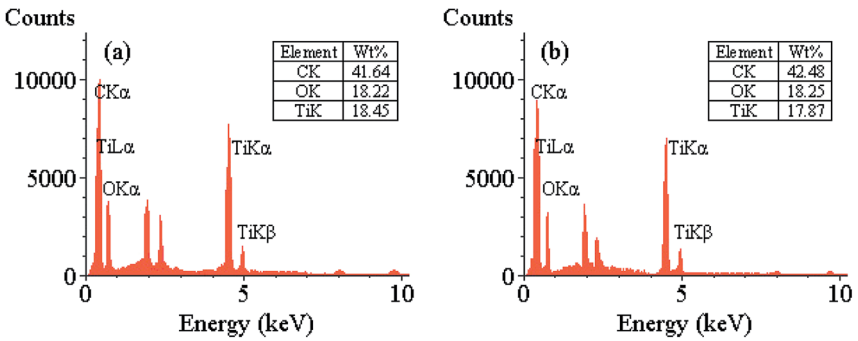

Fig. 6 The results of EDX analyses of TiO_2-CNTs nanocomposite (a) fresh catalyst, (b) 3rd recycle catalyst used.

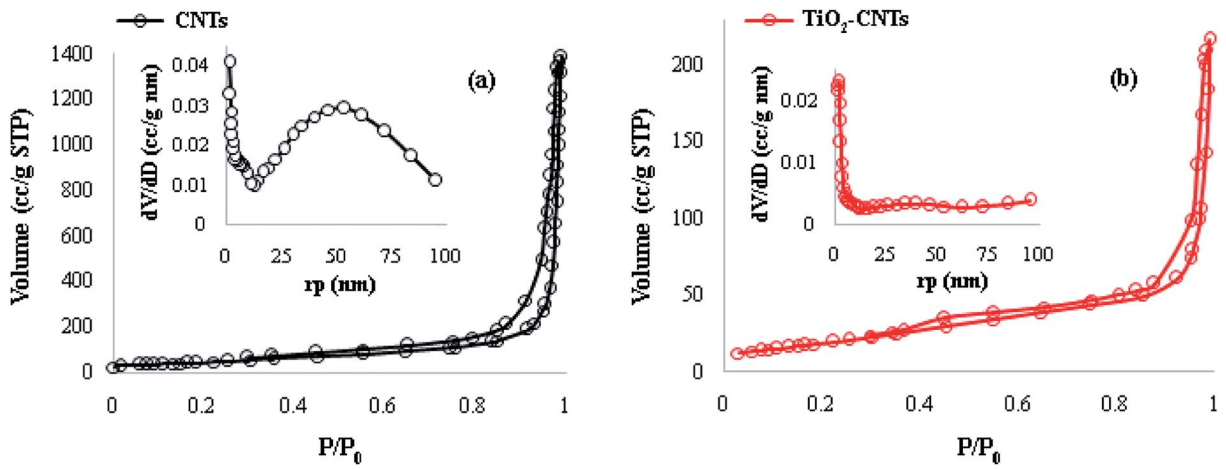

Fig. 7 N_2 adsorption–desorption isotherms of the (a) CNTs, (b) TiO_2-CNTs.

NH_2), 7.72 (1H, t, J = 8.1 Hz, H_{Ar}), 7.92 (1H, d, J = 8.0 Hz, H_{Ar}) ppm. ^{13}C NMR (125 MHz, DMSO-d_6): δ 77.2, 103.6, 113.7, 115.1, 117.4, 119.4, 123.5, 127.6, 132.8, 134.0, 140.6, 141.4, 143.9, 150.1, 153.1, 161.1, 169.3 ppm. Anal. calcd for $C_{17}H_9N_3O_2S$ (319.34): C, 63.94; H, 2.84; N, 13.16. Found: C, 64.10; H, 2.92; N, 13.04.

3. Results and discussions

Firstly, TiO_2-CNTs nanocomposite was prepared *via* a sonochemical approach based on the work of Salavati-Niasari *et al.*[58] The XRD pattern of CNTs, TiO_2 NPs, and TiO_2-CNTs nanocomposite is shown in Fig. 2. All reflection peaks in Fig. 2 can be readily indexed to the anatase phase of TiO_2 in the nanocomposite. Accordingly, the position of the main peaks of CNTs such as the strong diffraction peaks at 2θ = 26.0° and 43.4° are so close to those of TiO_2, which could cause to overlap the CNTs peaks by TiO_2, it should be noted that these peaks are not observed in the XRD patterns.[59]

Size and morphology of the as-prepared TiO_2-CNTs nanocomposite were characterized by the SEM and TEM images as depicted in Fig. 3 and 4 respectively. The SEM study reveals a continuous and mesoporous distribution of TiO_2 in the form of anatase bonding to the outer surface of CNTs (Fig. 3).

The average particle size of TiO_2 NPs was measured by the TEM analysis to have about 16–18 nm dimensions (Fig. 4). The TEM image of CNTs also shows that CNTs are multi-walled nanotubes with the inner diameter about 12–15 nm (Fig. 5). The prepared nanocomposite was also elemental analyzed by EDX (Fig. 6a). The results show that the weight ratio is almost 50 : 50.

The specific surface area and pore size distribution of CNTs and TiO_2-CNTs nanocomposites were determined from the

Table 1 Results of BET analyses for CNTs and TiO_2-CNTs

Sample	BET surface area ($m^2\ g^{-1}$)	Total pore volume ($cm^3\ g^{-1}$)	Mean pore diameter (nm)
CNTs	156.32	2.31	58.43
TiO_2-CNTs	65.97	0.38	21.67

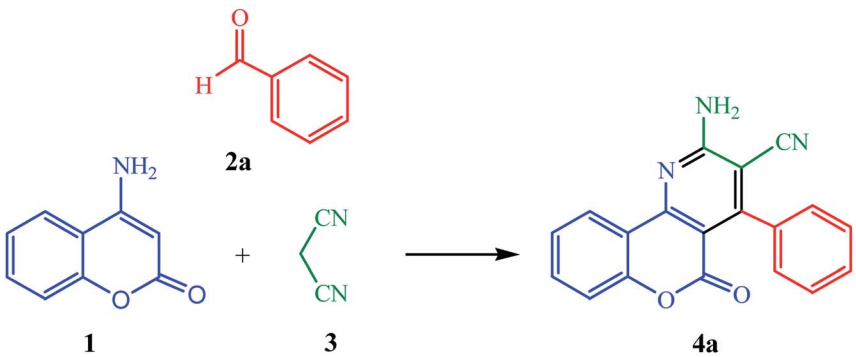

Scheme 2 Synthesis of 2-amino-5-oxo-4-phenyl-5*H*-chromeno[4,3-*b*]pyridin-3-yl cyanide (**4a**) as model reaction for the screening of the optimized reaction conditions.

Table 2 Optimization of reaction conditions for the synthesis of 2-amino-5-oxo-4-phenyl-5*H*-chromeno[4,3-*b*]pyridin-3-yl cyanide (**4a**)

Entry	Catalyst (g)	Solvent (conditions)	US power[a] (W)	Time (min)	Yield[b,c] (%)
1	—	H_2O (US)	60	40	56
2	TiO_2-CNTs (0.01)	H_2O (US)	60	30	82
3	TiO_2-CNTs (0.02)	H_2O (US)	60	20	94
4	TiO_2-CNTs (0.03)	H_2O (US)	60	20	90
5	TiO_2 NPs (0.02)	H_2O (US)	60	20	79
6	TiO_2 bulk (0.02)	H_2O (US)	60	20	67
7	MWCNTs (0.02)	H_2O (US)	60	20	33
8	TiO_2-CNTs (0.02)	H_2O (RT)	—	300	74
9	TiO_2-CNTs (0.02)	H_2O (reflux)	—	120	89
10	TiO_2-CNTs (0.02)	EtOH (US)	60	20	86
11	TiO_2-CNTs (0.02)	CH_2CL_2 (US)	60	20	75
12	TiO_2-CNTs (0.02)	CH_3CN (US)	60	20	83
13	TiO_2-CNTs (0.02)	DMF (US)	60	20	68
14	TiO_2-CNTs (0.02)	H_2O (US)	50	20	90
15	TiO_2-CNTs (0.02)	H_2O (US)	70	20	94

[a] US: ultrasonic irradiation. [b] Isolated yield. [c] Reaction conditions: a mixture of 4-aminocoumarin (**1**, 1 mmol), benzaldehyde (**2a**, 1 mmol), and malononitrile (**3**, 1.2 mmol) were kept at various reaction conditions.

nitrogen adsorption/desorption isotherm curves (Fig. 7). The BET analyses for CNTs and TiO_2-CNTs nanocomposite are also summarized in Table 1. The results indicate that the average pore diameter is reduced with the growth of CNTs over TiO_2 NPs.

In this study, we sought to develop a simple and efficient route which allows reuse of catalyst for several times. We tried to focus on a model reaction between 4-aminocoumarin (**1**), benzaldehyde (**2a**), and malononitrile (**3**) for the synthesis of specific product **1a** under various reaction conditions (Scheme 2 and Table 2). The preliminary experiments demonstrated that the conversion of the reactants into the desired product (**4a**) is mainly affected by using of TiO_2-CNTs nanocomposite as catalyst. Further research on the optimal quantity of the catalyst showed that 0.03 g of catalyst, does not increase the yield of reaction (Table 2, entry 4), and this is probably because of a further amount of catalyst, can decompose the product to initial molecules. As a result, only 0.02 g of the nanocomposite was efficient to push the reaction forward in water and under ultrasonic irradiation (Table 2, entries 1–4). Whereas replacing the TiO_2-CNTs nanocomposite with the bare TiO_2 NPs (0.02 g), TiO_2 bulk (0.02 g), and CNTs (0.02 g) under the same conditions, resulted in lower yields (Table 2, entries 3 and 5–7). In the next run of experiments, we used 0.02 g of the nanocomposite

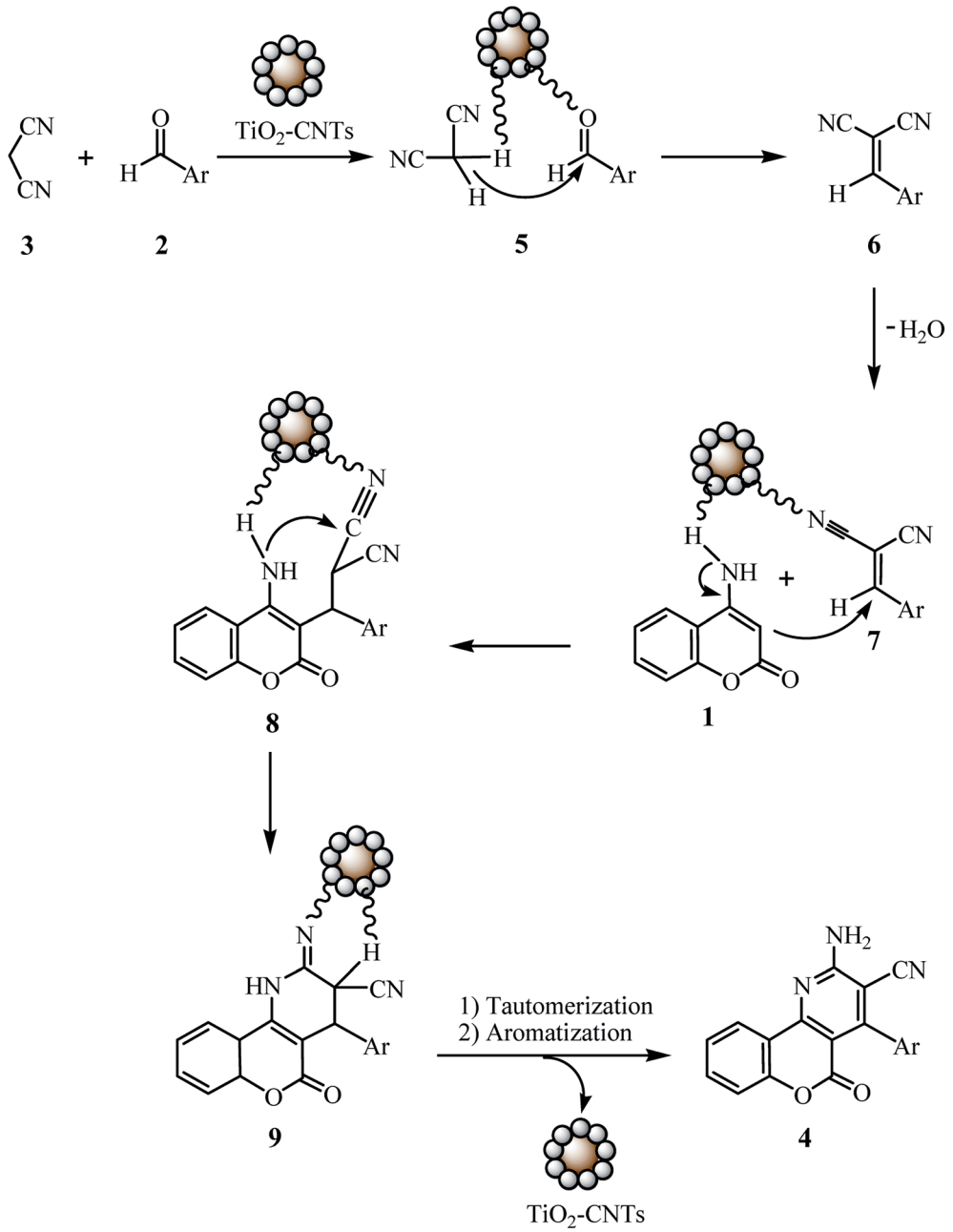

Scheme 3 The proposed mechanism for the formation of **4**.

for the model reaction in water and at two different conditions involving room temperature and under reflux conditions. Interestingly, the ultrasonic irradiation allowed the catalyst to exhibit higher reactivity (Table 2, entries 3 and 8–9). In evaluating the effect of the reaction media, several solvents including, EtOH, CH_2CL_2, CH_3CN, and DMF were tested. Results indicated that the performing reaction in water was afforded the best yield of product (94%) within 20 min. The power of ultrasonic irradiation was the last component which was explored. However, the promising results were obtained in power of 60 W (Table 2, entries 3, 14 and 15).

After completion of the model reaction, the catalyst was recovered successfully by a simple manner as described in the general procedure and subjected subsequently to at least four consecutive experiments without significant loss of activity (Scheme 3 and Table 3). From the EDX images of the fresh and third recycled catalyst reuse, the elemental structure and percentage of TiO_2-CNTs nanocomposite as expected haven't changed and could be compared after and before catalysis (Fig. 6).

The scope and limitation of this protocol was explored by treating a range of various substituted benzaldehydes and heteroaromatic aldehydes with 4-aminocoumarin and malononitrile to form the corresponding products in high yields which were conducted under optimized reaction conditions (Table 4).

The structures of compounds **4(a–l)** were confirmed by IR, ^{1}H NMR and ^{13}C NMR spectroscopic data and also by elemental analyses. Spectroscopic data have been given in the Experimental Section. The synthesized catalyst was fully characterized by XRD, SEM, TEM, and EDX techniques.

Although the catalytic role of CNTs have not been proved in organic reactions, however, it is worth noting that the electron-accepting capability and conductivity of CNTs make them appropriate support to improve the conductive and dielectric properties of TiO_2 NPs. In this manner, and according to the comparison as noted in entries 3, 5, and 7 in Table 2, which shows that the main catalytic role has been played by TiO_2 in nanocomposite, a possible mechanism for the formation of **4** is illustrated in Scheme 2. First, TiO_2 nanoparticles can act as Lewis acid–base catalyst to generate alkene **7** through the Knoevenagel condensation between aromatic aldehyde **3** and malononitrile **2**. The subsequent Michael addition of 4-aminocoumarin **1** to alkene **7** is also catalyzed by TiO_2 nanoparticles to form Micheal adduct **8**. Further cycloaddition of amino group to the cyano moiety in intermediate **9** provides the desired product **4** after tautomerization and aromatization. In order to support experimentally the proposed mechanism, we also examined the same reaction for the synthesis **1a**, in two separate steps. At first benzaldehyde (**2a**), and malononitrile (**3**) were reacted together using TiO_2-CNTs (0.02 g) in the absence of 4-aminocoumarin (**1**). The obtained alkene **7a** as solid white with mp = 87 °C (lit: 85 °C),[60] was the same intermediate which was indicated on TLC in tree–component reaction. When the resulted alkene **7a** reacts with 4-aminocoumarin (**1**) in the second step, the resulted product was exactly the same as the one obtained in one-step route.

Table 3 Recyclability of TiO_2-CNTs for the synthesis of 2-amino-5-oxo-4-phenyl-5*H*-chromeno[4,3-*b*]pyridin-3-yl cyanide (**4a**) under optimized reaction conditions

Run	Fresh	1	2	3	4
Isolated yield (%)[a,b]	94	94	93	93	92

[a] Isolated yield. [b] Reaction conditions: a mixture of 4-aminocoumarin (**1**, 1 mmol), benzaldehyde (**2a**, 1 mmol), malononitrile (**3**, 1.2 mmol), and in H_2O (3 mL) TiO_2-CNTs nanocomposite (0.02 g) in H_2O (3 mL) was sonicated at room temperature for 20 min at power of 60 W.

Table 4 TiO_2-CNTs nanocomposite catalyzed synthesis of 2-amino-5-oxo-4-aryl-5*H*-chromeno[4,3-*b*]pyridin-3-yl cyanides **4a–l** under ultrasonic irradiation in water

Products	Ar	Yield[a,b] (%)	Mp (°C)
4a	C_6H_5	94	302–304
4b	3-Cl–C_6H_4	93	287–289
4c	2,4-Cl_2–C_6H_3	93	296–298
4d	4-NC–C_6H_4	95	300–302
4e	4-F–C_6H_4	96	256–258
4f	3-HO–C_6H_4	94	292–294
4g	4-HO–C_6H_4	95	285–287
4h	4-CH_3O–C_6H_4	96	278–280
4i	4-CH_3–C_6H_4	95	291–2193
4j	3-O_2N–C_6H_4	96	284–286
4k	Pyridin-4-yl	96	289–291
4l	Thiophen-2-yl	95	280–282

[a] Yields refer to those of pure isolated products characterized by IR, ^{1}H NMR and ^{13}C NMR spectral data and by elemental analyses. [b] Reaction conditions: a mixture of 4-aminocoumarin (**1**, 1 mmol), aromatic aldehyde **2** (1 mmol), malononitrile (**3**, 1.2 mmol), and in H_2O (3 mL) TiO_2-CNTs nanocomposite (0.02 g) in H_2O (3 mL) was sonicated at room temperature for 20 min at power of 60.

4. Conclusion

In summary, we have reported an experimentally simple and expeditious approach to synthesize a series of chromeno[*b*] pyridine derivatives using 4-aminocoumarin, aromatic aldehydes, and malononitrile as substrates and TiO_2-CNTs as a catalyst. This protocol offers several advantages including high yields, short reaction time, an easy work-up procedure, and catalyst reusability for several runs. It also has the ability to tolerate the use of heteroaromatic aldehydes as well as various substituted benzaldehydes.

Conflicts of interest

There are no conflicts to declare.

Acknowledgements

Shahrzad Abdolmohammadi is grateful to the Research Council of East Tehran Branch, Islamic Azad University, for financial support.

References

1 R. Pratap and V. J. Ram, *Chem. Rev.*, 2014, **114**, 10476–10526.
2 G. P. Ellis, *The Chemistry of Heterocyclic Compounds Chromenes, Chromanes and Chromones*, ed. A.Weissberger and E. C.Taylor, John Wiley, New York, 1977, ch. 2, pp. 11–139.
3 E. A. A. Hafez, M. H. Elnagdi, A. G. A. Elagamey and F. M. A. A. El-Taweel, *Heterocycles*, 1987, **26**, 903–907.
4 M. M. Khafagy, A. H. Abd el-Wahab, F. A. Eid and A. M. el-Agrody, *Farmaco*, 2002, **57**, 715–722.
5 W. P. Smith, L. S. Sollis, D. P. Howes, C. P. Cherry, D. I. Starkey and N. K. Cobley, *J. Med. Chem.*, 1998, **41**, 787–797.
6 A. Martinez-Grau and J. L. Marco, *Bioorg. Med. Chem. Lett.*, 1997, **7**, 3165–3170.
7 S. J. Mohr, M. A. Chirigos, F. S. Fuhrman and J. W. Pryor, *Cancer Res.*, 1975, **35**, 3750–3754.
8 K. Hiramoto, A. Nasuhara, K. Michiloshi, T. Kato and K. Kikugawa, *Mutat. Res.*, 1997, **395**, 47–56.
9 C. P. Dell and C. W. Smith, European patent applications EP 537949, 21 Apr 1993Chem. Abstr., 119, 1993, 139102d.
10 G. Bianchi and A. Tava, *Agric. Biol. Chem.*, 1987, **51**, 2001–2002.
11 K. Mukai, K. Okabe and H. Hosose, *J. Org. Chem.*, 1989, **54**, 557–560.
12 T. Ishikawa, *Heterocycles*, 2000, **53**, 453–474.
13 F. Eiden and F. Denk, *Arch. Pharm.*, 1991, **324**, 353–354.
14 C. D. Hufford, B. O. Oguntimein, D. Van Engen, D. Muthard and J. Clardy, *J. Am. Chem. Soc.*, 1980, **102**, 7365–7367.
15 V. Fuendjiep, A. E. Nkengfack, Z. T. Fomum, B. L. Sondengam and B. Bodo, *J. Nat. Prod.*, 1998, **61**, 380–383.
16 J. Jean Wandji, Z. T. Fomum, F. Tillequin, F. Libot and M. Koch, *J. Nat. Prod.*, 1995, **58**, 105–108.
17 C. Burda, X. B. Chen, R. Narayanan and M. A. El-Sayed, *Chem. Rev.*, 2005, **105**, 1025–1102.
18 A. Y. Kim, H. J. Lee, J. C. Park, H. Kang, H. Yang, H. Song and K. H. Park, *Molecules*, 2009, **14**, 5169–5178.
19 K. S. Lin, C. Y. Pan, S. Chowdhury, M. T. Tu, W. T. Hong and C. T. Yeh, *Molecules*, 2011, **16**, 348–366.
20 A. Monopoli, A. Nacci, V. Caló, F. Ciminale, P. Cotugno, A. Mangone, L. C. Giannossa, P. Azzone and N. Cioffi, *Molecules*, 2010, **15**, 4511–4525.
21 M. L. Kantam, S. Laha, J. Yadav and B. Sreedhar, *Tetrahedron Lett.*, 2006, **47**, 6213–6216.
22 M. Hosseini-Sarvari, *Acta Chim. Slov.*, 2007, **54**, 354–359.
23 J. L. Ropero-Vega, A. Aldana-Péreza, R. Gómez and M. E. Niño-Gómez, *Appl. Catal., A*, 2010, **379**, 24–29.
24 M. Z. Kassaee, R. Mohammadi, H. Masrouri and F. Movahedi, *Chin. Chem. Lett.*, 2011, **22**, 1203–1206.
25 F. Shirini, M. Alipour Khoshdel, M. Abedini and S. V. Atghia, *Chin. Chem. Lett.*, 2011, **22**, 1211–1214.
26 F. Shirini, S. V. Atghia and M. Alipour Khoshdel, *Iran. J. Catal.*, 2011, **1**, 93–97.
27 S. M. Sajadi, M. Naderi and S. Babadoust, *J. Nat. Sci. Res.*, 2011, **1**, 10–17.
28 S. Abdolmohammadi, *Chin. Chem. Lett.*, 2012, **23**, 1003–1006.
29 S. Iijima, *Nature*, 1991, **354**, 56–58.
30 E. Auer, A. Freund, J. Pietsch and T. Tacke, *Appl. Catal., A*, 1998, **173**, 259–271.
31 K. Woan, G. Pyrgiotakis and W. Sigmund, *Adv. Mater.*, 2009, **21**, 2233–2239.
32 J. Safari and S. Gandomi-Ravandi, *J. Mol. Struct.*, 2014, **1065**, 241–247.
33 I. Horvath and P. Anastas, *Chem. Rev.*, 2007, **107**, 2167–2168.
34 S. L. Schreiber, *Nature*, 2009, **457**, 153–154.
35 J. Zhu and H. Bienaymé, *Multicomponent Reactions*, Wiley-VCH, Weinheim, 2005.
36 B. M. Trost, *Acc. Chem. Res.*, 2002, **35**, 695–705.
37 P. A. Wender, V. A. Verma, T. J. Paxton and T. H. Pillow, *Acc. Chem. Res.*, 2008, **41**, 40–49.
38 S. Farshbaf, L. Sreerama, T. Khodayari and E. Vessally, *Chem. Rev. Lett.*, 2018, **1**, 56–67.
39 F. Behmagham, Z. Asadi and Y. J. Sadeghi, *Chem. Rev. Lett.*, 2018, **1**, 68–76.
40 M. Nikpassand and L. ZareFekri, *Chem. Rev. Lett.*, 2019, **2**, 7–12.
41 F. Valinia, N. Shojaei and P. Ojaghloo, *Chem. Rev. Lett.*, 2019, **2**, 90–97.
42 E. Jafari, P. Farajzadeh, N. Akbari and A. Karbakhshzadeh, *Chem. Rev. Lett.*, 2019, **2**, 123–129.
43 N. Parikh, D. Kumar, S. R. Roy and A. K. Chakraborti, *Chem. Commun.*, 2011, **47**, 1797–1799.
44 G. Sharma, R. Kumar and A. K. Chakraborti, *Tetrahedron Lett.*, 2008, **49**, 4269–4271.
45 A. K. Chakraborti, S. Rudrawar, K. B. Jadhav, G. Kaur and S. V. Chankeshwara, *Green Chem.*, 2007, **9**, 1335–1340.
46 S. V. Chankeshwara and A. K. Chakraborti, *Org. Lett.*, 2006, **8**, 3259–3262.
47 G. L. Khatik, R. Kumar and A. K. Chakraborti, *Org. Lett.*, 2006, **8**, 2433–2436.
48 B. A. Song, G. P. Zhang, S. Yang, D. Y. Hu and L. H. Jin, *Ultrason. Sonochem.*, 2006, **13**, 139–142.
49 T. J. Mason, *Chem. Soc. Rev.*, 1997, **26**, 443–451.
50 R. Mawson, M. Gamage, N. S. Terefe and K. Knoerzer, *Ultrasound Technol. Food Bioprocess.*, 2011, pp. 369–404.
51 Y. Q. Liu, L. H. Li, L. Yang and H. Y. Li, *Chem. Pap.*, 2010, **64**, 533–536.
52 M. Meciarova, V. Polackova and S. Toma, *Chem. Pap.*, 2002, **56**, 208–213.
53 M. Meciarova, S. Toma and P. Babiak, *Chem. Pap.*, 2004, **58**, 104–108.
54 K. Tabatabaeian, M. Mamaghani, N. O. Mahmoodi and A. Khorshidi, *Catal. Commun.*, 2008, **9**, 416–420.
55 S. Khalilian, S. Abdolmohammadi and F. Nematolahi, *Lett. Org. Chem.*, 2017, **14**, 361–367.
56 A. Samani, S. Abdolmohammadi and A. Otaredi-Kashani, *High-Throughput Screening*, 2018, **21**, 111–116.
57 S. Abdolmohammadi, *Comb. Chem. High Throughput Screening*, 2018, **21**, 594–601.
58 E. Khosravifard, M. Salavati-Niasari, M. Dadkhah and Gh. Sodeifian, *J. Nanostruct.*, 2012, **2**, 191–197.
59 B. Gao, G. Z. Chen and G. L. Puma, *Appl. Catal., B*, 2009, **89**, 503–509.
60 S. Balalaie and N. Nemati, *Synth. Commun.*, 2000, **30**, 869–875.

